

## Phytoplankton Populations in the Western Bransfield Strait and the Southern Drake Passage, Antarctica

Kang, Sung-Ho, Moon Sik Suk\*, Chang Soo Chung\*\*,  
Soo Yong Nam\* and Cheon Yoon Kang

Polar Research Center, Korea Ocean Research & Development Institute (KORDI),  
Ansan P.O. Box 29, Seoul 425-600, Korea

\* Physical Oceanography Division, KORDI

\*\* Chemical Oceanography Division, KORDI

The quantitative composition, biomass and mesoscale distribution of phytoplankton were studied in the western Bransfield Strait region including the southern portion of Drake Passage during the austral summer (February) of 1993 as part of the 6th Korea Antarctic Research Program (KARP). Dominant phytoplankton species in terms of biomass (carbon) were phytoflagellates such as *Cryptomonas* sp. and *Phaeocystis* sp. (motile form) and diatoms such as *Fragilariopsis pseudonana* and *Rhizosolenia antennata* fo. *semispina*, accounting for about 87% of total phytoplankton carbon. The distribution and biomass of the phytoplankton populations within the study area were variable, with the higher total phytoplankton cell carbon values generally being found northern portion of the study area near Snow and Livingston Islands Shelves and in Drake Passage waters, while the lower values were generally in Bransfield Strait waters. Phytoflagellates and diatoms showed different distribution patterns. The relative and absolute values of carbon biomass of phytoflagellates were higher in Bransfield Strait region, while the diatoms were more dominant in the southern Drake Passage region. Principal component analysis (PCA) using cell carbon density of the dominant phytoplankton species ( $\mu\text{g}\cdot\text{C}\cdot\text{l}^{-1}$ ) from 144 discrete water samples as variables revealed that the samples from the western Bransfield Strait region were not only separated based on depth (above pycnocline vs. below pycnocline), but also separated based on horizontal water mass differences such as fine-scale temperature gradients between stations.

**Key words:** phytoplankton, composition, biomass, distribution, Bransfield Strait, Drake Passage

### INTRODUCTION

The primary producer phytoplankton which use energy from sunlight to convert carbon dioxide to biological material is the ultimate food source for nearly all biological communities in the Antarctic marine ecosystem. The decrease in total ozone content over Antarctica was notable during the 1980s (Fig. 1). The springtime ozone depletion in the lower stratosphere leads to a period with increased UV-B radiation flux on the Antarctic phytoplankton. Recent investigations indicate that Antarctic marine phytoplankton are presently UV-stressed (Karentz *et al.*, 1991; Smith *et al.*, 1992). The

extent to which increasing UV radiation diminishes the ability of phytoplankton to fix  $\text{CO}_2$  and/or leads to changes in their species composition is equivocal (Marchant and Davidson, 1992). If there are changes in the species composition of Antarctic phytoplankton, changes to trophic interactions are likely (Fig. 2).

A unique combination of geographical isolation and diverse environmental extremes has resulted in low phytoplankton species diversity in terms of biomass and resulted in distinctive Antarctic phytoplankton communities. Thus, the Antarctic phytoplankton can be used as sensitive monitors of environmental change and useful indicators of cumula-

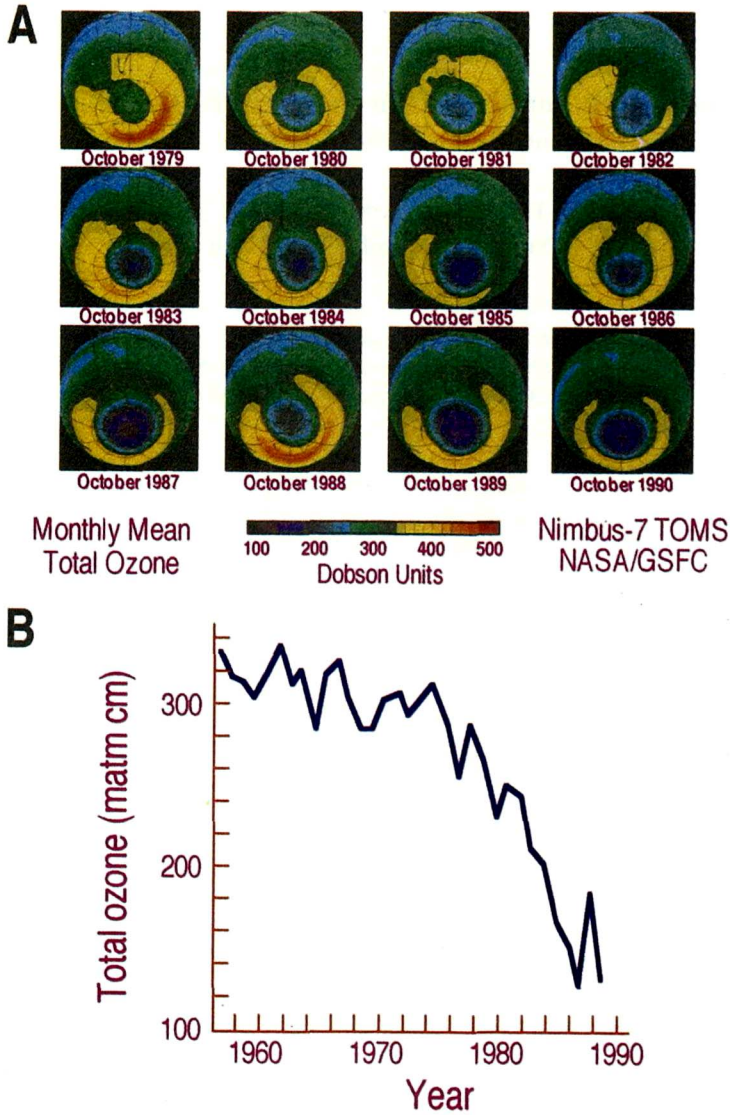


**Fig. 1.** (A) Total column ozone concentrations (in Dobson units) over Antarctica as determined by the TOMS (Total Ozone Monitoring Satellite) during October from 1979 to 1990. (National Aeronautics and Space Administration). (B) Monthly means of total ozone over Halley Bay, Antarctica, for October of the years 1957 through 1989. A layer of gaseous ozone 1 mm thick at 1 atmosphere pressure and 0°C corresponds to 100 matm cm. (Modified from figure 1.1 in Graedel, T. E. and P. J. Crutzen, 1993, *Atmospheric Change: An Earth System Perspective*, W. H. Freeman and Company, New York).

tive damage such as increased UV-B radiation damage.

It is important to know and find environmentally-sensitive species and their biomass and distribution patterns because the goals of Antarctic detection-of-change research should be to determine what is happening now throughout Antarctica and

the surrounding seas, attempt to relate the current situation to the past and understand why the changes are occurring. Numerous studies have found that the phytoplankton species composition and distribution show severe seasonal and regional variability. For example, in the ice-edge zones phytoplankton populations have been found to be dom-

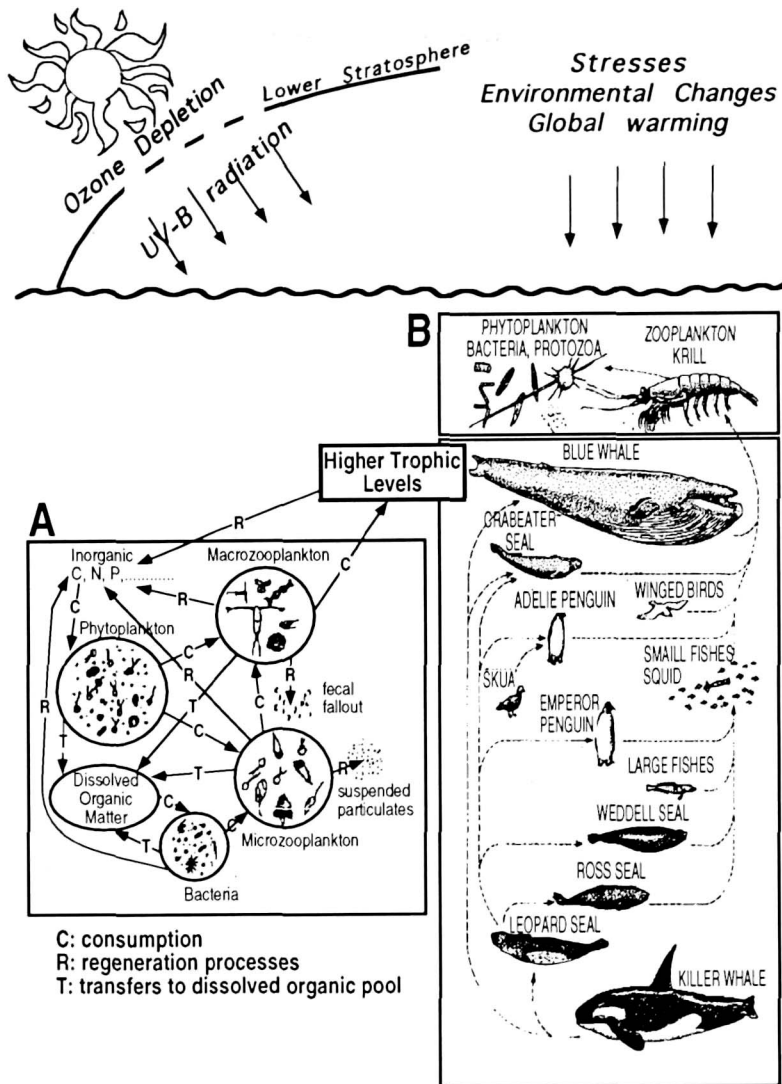


Fig. 2. Diagram of principal food-web connections in the Antarctic marine ecosystem which has been affected by environmental changes and stresses such as UV-B radiation. (A) Microbial loop. (B) Simplified food chain.

inated by *Phaeocystis* Lagerheim in colonial stage, *Fragilariopsis* Hustedt in Schmidt and *Pseudonitzschia* Peragallo (e.g. Garrison and Buck, 1985; Fryxell and Kendrick, 1988; Kang and Fryxell, 1992, 1993; Kang et al., 1993a). In the west of Antarctic Peninsula region *Cryptomonas* Ehrenberg, *Phaeocystis* Lagerheim in motile stage, picoplanktonic flagellates were dominant genera (e.g. Kocczynska, 1992; Becquevort et al., 1992). In areas of increased water column stability induced by ice melting and/or local atmospheric warming of water which was trapped around

islands and coastal area during austral summer, larger-celled diatoms such as *Rhizosolenia* Brightwell, *Corethron* Castracane, *Chaetoceros* Ehrenberg, and *Thalassiosira* Cleve were dominant genera (e.g. Kang and Fryxell, 1991; Leventer, 1991).

Although a number of previous studies on phytoplankton populations had conducted at or near the Bransfield Strait region, a little mesoscale study of a restricted geographical region had been investigated. The mesoscale study area during the 6th KARP cruise is characterized by complex physical circulation, involving waters from the coastal shelf,

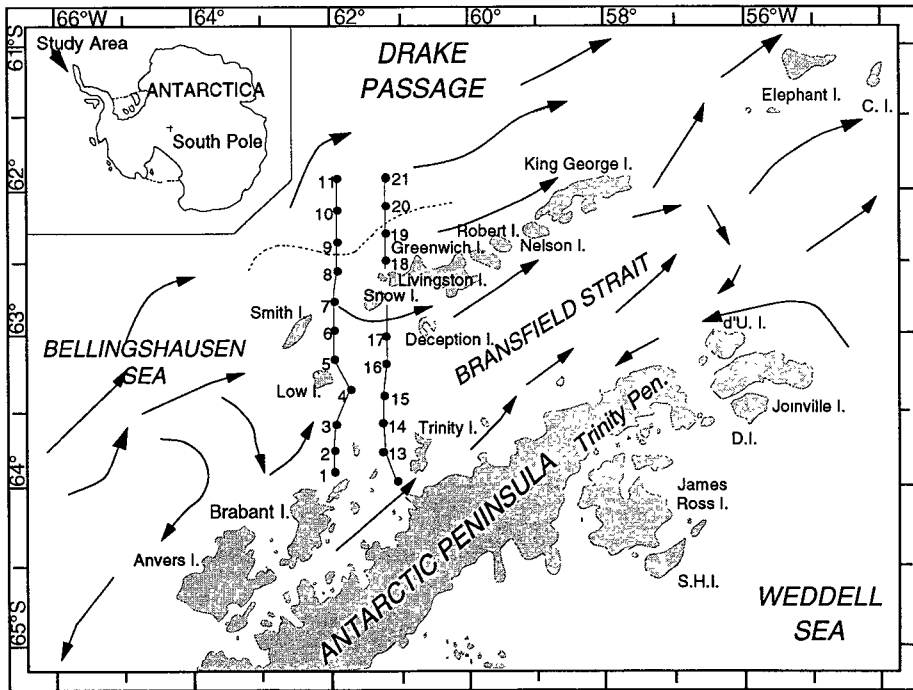


Fig. 3. Station locations during the 6th KARP cruise. All 21 stations were occupied during February 1993. The dashed line in Drake Passage indicates the location of the continental shelf break, north of which depths exceed 1000 m. Arrow lines indicate the main directions of water movement (after Hofmann *et al.*, 1992).

the continental shelf break, the island shelves, the Bellingshausen Sea-Weddell Sea confluence, and a portion of Drake Passage. The objective was to understand the structure of phytoplankton populations at one point in space and time in such a complex coastal environment.

## MATERIALS AND METHODS

Samples were collected during the 6th KARP cruise in the western Bransfield Strait region during February 5-7, 1993 at the locations showing in Fig. 3. Salinity and temperature profiles were determined with a Mark V CTD-profiler (General Oceanics products). A CTD/rosette unit was used at all stations for vertical profiles of the physical characteristics of the water column and to collect water samples. The discrete water samples were collected at 7 depths (0, 10, 20, 30, 50, 75, and 100 m) in the upper 100 m using 5-liter PVC Niskin bottles. Aliquots of 125 ml were preserved with glutaraldehyde-25% (final concentration 1%). Phytoplankton net tows (20- $\mu$ m mesh) were taken and

preserved with glutaraldehyde-25% (final concentration 2%). These concentrated samples enabled us to examine the rarer components of the phytoplankton.

Membrane filter mount technique was used for absolute cell counts to gain quantitative information on the composition, abundance and distribution of phytoplankton species. The membrane filter mount technique with water-soluble embedding medium (HPMA, 2-hydroxypropyl methacrylate) using filtered samples described by Crumpton (1987) has shown many advantages to be used for phytoplankton quantitative analysis: 1) Resulting mounts are relatively permanent at least six years in our storage condition, and thus provide a long-term record of the sample. 2) The technique is ideal for making accurate quantitative estimates of pico- and nanoplanktonic phytoplankton that can be distinguished by morphological characteristics on a light microscope using multiple optical modes of contrast and by a epifluorescence microscope. It is possible to differentiate autotrophic and heterotrophic protists because the HPMA-mounted

phytoplankton cells autofluoresce under epifluorescence microscope. The HPMA slides made in six years ago and stored in room temperature for six year still clearly autofluoresce (personal observation).

Sample volume of 50 to 100 ml was filtered on board ship depending on the expected density of phytoplankton and the HPMA slides were made for cell counts. At least 300 cells were enumerated using a Zeiss Axiophot microscope, with combination of light and epifluorescence microscopy at 400x for microplankton and at 1000x for pico- and nanoplankton. For species identification which was not possible under the light microscope, a Philips 515 scanning electron microscope (Polar Research Center, KORDI) was used. Pico- and nanoplanktonic phytoflagellates were filtered, dehydrated and critical point-dried according to standard methods (Dykstra 1992). Whole mounts coated with gold were used for the scanning electron microscopy.

The number of phytoplankton cells per liter of sea water was obtained by counting numbers of cells per unit area, corrected for total area and volume used, calculated as in Kang (1989) and Kang and Fryxell (1991) from raw microscope counts. Cell sizes and areas of dominant phytoplankton species were measured for subsequent biovolume and carbon biomass estimates. Carbon biomass was estimated from cell biovolume with the modified Strathmann equations (Eqs. 7 and 8 in Smayda 1978). For autotrophic flagellates, the relationship  $\log_{10} \text{carbon}(\text{pg}) = 0.94 \cdot \log_{10} [\text{cell volume}(\mu\text{m}^3)] - 0.60$  was used, and for diatoms the relationship  $\log_{10} \text{carbon}(\text{pg}) = 0.76 \cdot \log_{10} [\text{cell volume}(\mu\text{m}^3)] - 0.352$ . The quantitative estimates of the abundant components of the phytoplankton were compared to assess variation with depth and variation between stations. The principal component analysis (PCA) was done with the SYSTAT for Macintosh and is based on the covariance matrix.

Nomenclature follows Hasle (1965a, b, 1972, 1993), Medlin and Priddle (1990) and Round et al. (1990), with recognition of *Cylindrotheca*, *Fragilariopsis*, *Pseudonitzschia* and *Nitzschia* as different genera in the family Bacillariaceae.

## RESULTS

### Dominant Species Composition

Examination of dominant phytoplankton species during the study period showed that the main components of the total phytoplankton carbon biomass were diatoms and phytoflagellates (Table 1). The dominant diatoms were *Chaetoceros*, *Corethron*, *Fragilariopsis*, *Pseudonitzschia* and *Rhizosolenia* species. These included mainly *Chaetoceros criophilum* Castracane, *Corethron criophilum* Castracane, *Fragilariopsis curta* (van Heurck) Hustedt, *F. cylindrus* (Grunow) Krieger in Helmcke and Kriger, *F. pseudonana* (Hasle) Hasle, *Pseudonitzschia lineola* (Cleve) Hasle, *P. prolongatoides* (Hasle) Hasle and *Rhizosolenia antennata* fo. *semispina* Sundström.

Cryptophytes, prymnesiophytes, a small (~1.5  $\mu\text{m}$ ) unidentified picoplankter, siliceous cysts (chrysophytes) and dinoflagellates (in order of decreasing biomass) comprised the important autotrophic phytoflagellates. *Cryptomonas* Ehrenberg sp. and *Phaeocystis* Lagerheim sp. in motile stage were the most dominant species within the phytoflagellate group.

### Standing Stock

The standing stock results, as measured by cell counts, and the relative contribution of the dominant phytoplankton species to the standing stock are presented in Table 1. Integrated total phytoplankton carbon in the upper 100 m of water column ranged from 500 to 3500  $\text{mg}\cdot\text{C}\cdot\text{m}^{-2}$ . Mean integrated total phytoplankton carbon was 1907  $\text{mg}\cdot\text{C}\cdot\text{m}^{-2}$ . Phytoflagellates and diatoms accounted for 60 % (1145  $\text{mg}\cdot\text{C}\cdot\text{m}^{-2}$ ) and 40 % (762  $\text{mg}\cdot\text{C}\cdot\text{m}^{-2}$ ) of the total phytoplankton carbon, respectively.

Only four phytoplankton species (*Cryptomonas* sp., *Fragilariopsis pseudonana*, *Phaeocystis* sp. (motile form), and *Rhizosolenia antennata* fo. *semispina* in order of decreasing order) accounted for about 87% of total phytoplankton carbon. Cryptophyte, *C. sp.* (Fig. 4A-C) was the most important carbon contributor, accounting for 708  $\text{mg}\cdot\text{C}\cdot\text{m}^{-2}$  (~37% of the total phytoplankton carbon; see Table 1). Pennate diatom, *F. pseudonana* (Fig. 5E-G), prymnesiophyte, *P. sp.* in motile stage (Fig. 4D-J) and centric diatom, *R. antennata* fo. *semispina* (Fig. 5A-C) accounted for 491  $\text{mg}\cdot\text{C}\cdot\text{m}^{-2}$  (~26%), 256  $\text{mg}\cdot\text{C}\cdot\text{m}^{-2}$  (~13%) and 201  $\text{mg}\cdot\text{C}\cdot\text{m}^{-2}$  (~11%) of the total phytoplankton carbon, respectively.

**Table 1.** Phytoplankton composition, average carbon (integrated mg-C-m<sup>-2</sup>), and relative carbon biomass in water column in the western Bransfield Strait region during the 6th KARP cruise, determined from microscopic examination. All estimates were integrated in the upper 100 m

Group/species	Mean Carbon (mg-C-m <sup>-2</sup> )	Relative Biomass (%)
<b>Diatoms:</b>		
<i>Asteromphalus hyalinus</i> Karsten	6.03	0.3
<i>Chaetoceros atlanticus</i> Cleve	< 0.1	< 0.1
<i>Ch. criophilum</i> Castracane	4.24	0.2
<i>Ch. dictyota</i> Ehrenberg	< 0.1	< 0.1
<i>Cocconeis fasciolata</i> (Ehrenberg) Brown	< 0.1	< 0.1
<i>Corethron criophilum</i> Castracane	2.69	0.14
<i>Cylindrotheca closterium</i> (Ehrenberg) Reimann & Lewin	< 0.1	< 0.1
<i>Fragilariopsis curta</i> (Van Heurck) Hustedt	0.54	< 0.1
<i>F. cylindrus</i> (Grunow) Krieger in Helmcke & Krieger	1.74	< 0.1
<i>F. pseudonana</i> (Hasle) Hasle	491.45	25.8
<i>F. rhombica</i> (O'Meara) Hustedt	< 0.1	< 0.1
<i>F. ritscheri</i> Hustedt	< 0.1	< 0.1
<i>F. spp.</i> (>10µm)	53.9	2.8
<i>Navicula spp.</i>	< 0.1	< 0.1
<i>Nitzschia lecointei</i> Van Heurck	< 0.1	< 0.1
<i>N. spp.</i>	< 0.1	< 0.1
<i>Proboscia alata</i> (Brightwell) Sundström	< 0.1	< 0.1
<i>Pseudonitzschia lineola</i> (Cleve) Hasle	0.25	< 0.1
<i>Pseudonitzschia prolongatoides</i> (Hasle) Hasle	0.13	< 0.1
<i>Rhizosolenia antennata</i> f. <i>semispina</i> Sundström	200.7	10.5
<i>Thalassiosira gracilis</i> v. <i>expecta</i> (Van Landingham) Fryxell & Hasle	< 0.1	< 0.1
<i>Th. spp.</i>	< 0.1	< 0.1
<i>Thalassiothrix spp.</i>	< 0.1	< 0.1
<b>Total Diatoms</b>	762	40.0
<b>Autotrophic flagellates:</b>		
<i>Amphidinium spp.</i>	< 0.1	< 0.1
<i>Cryptomonas sp.</i>	708.1	37.1
cysts	19.0	1.0
<i>Distephanus speculum</i> (Ehrenberg) Haeckel	< 0.1	< 0.1
<i>Gymmodinium spp.</i>	< 0.1	< 0.1
<i>Phaeocystis sp.</i> (motile)	255.8	13.4
<i>Prorocentrum spp.</i>	8.8	0.46
<i>Pyraminonas spp.</i>	< 0.1	< 0.1
Unid. dinoflagellates	< 0.1	< 0.1
Unid. flagellates (about 5 µm)	43.6	2.3
Unid. flagellate (about 1 µm)	109.0	5.7
<b>Total Phytoflagellates</b>	1145	60.0
<b>Total Phytoplankton</b>	1907	

### Mesoscale Distribution Patterns

Horizontal and vertical phytoplankton distributions were obtained from two north-south transects.

Fig. 6 is contour plots of carbon values on total phytoplankton, total phytoflagellates, and total diatoms. Fig. 7 is contour plots of the dominant species such as *Cryptomonas sp.*, *Phaeocystis sp.*

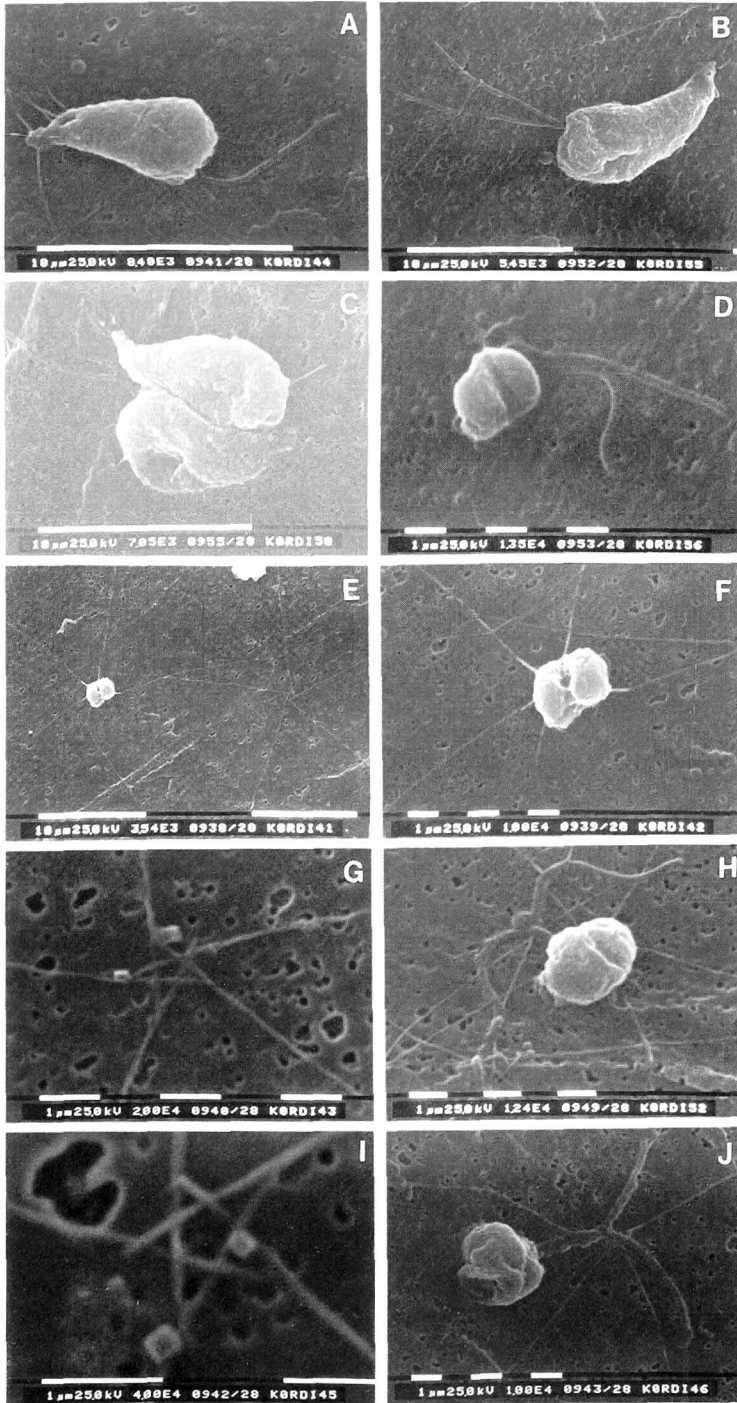


**Fig. 4.** Scanning electron micrographs (SEM) of critical-point-dried cells of *Cryptomonas* sp. showing the two flagella arising laterally from a subapical mound (A, B). Two dividing cells (C). *Phaeocystis* sp. (motile stage) showing *Phaeocystis* cells lying on thread-like material (E, F, H) with flagella (D, H, J); note the pentagonal structure of the thread-like material (G, I).

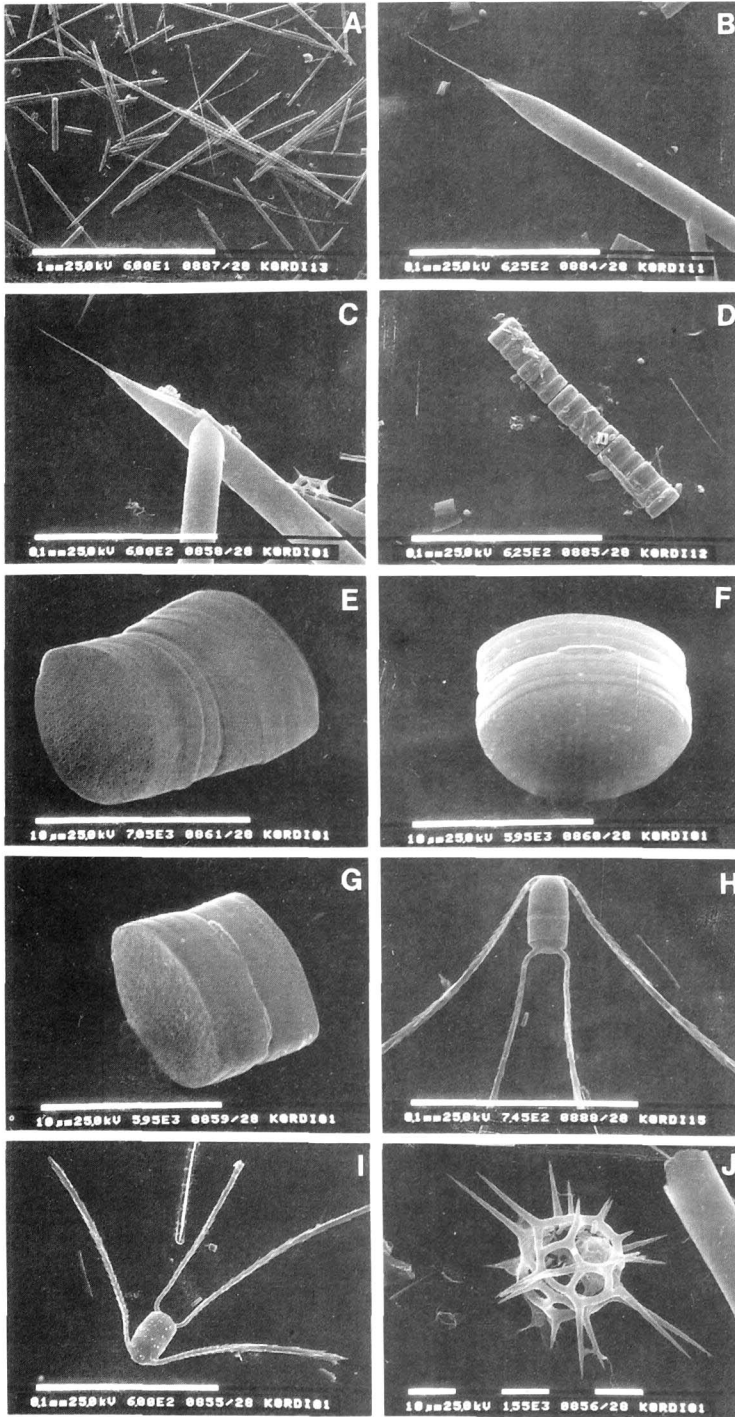
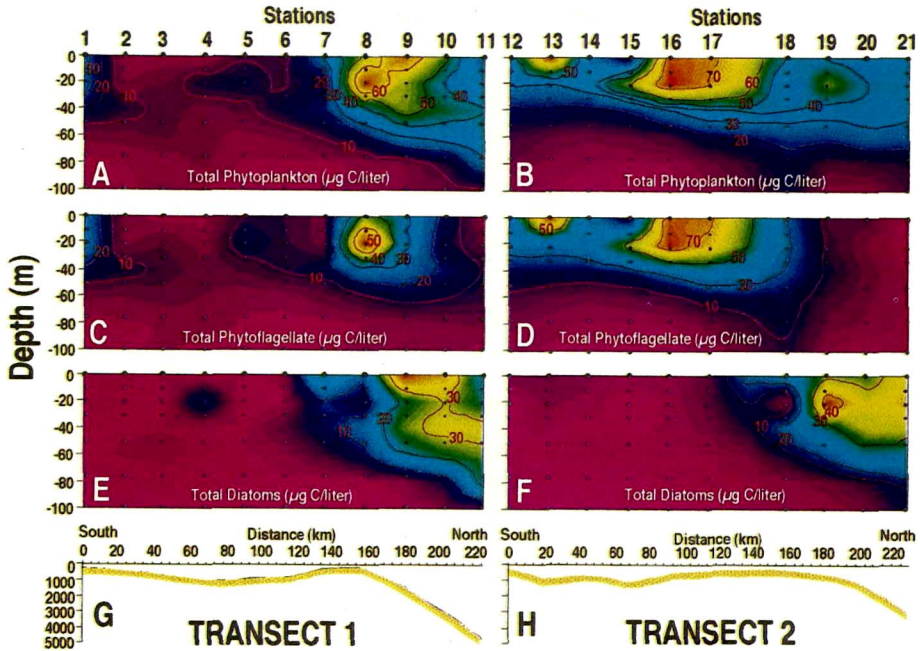


Fig. 5. Scanning electron micrographs (SEM) of *Rhizosolenia antennata* f. *semispina* from net materials (A-C). *Fragilariopsis* sp. forming colony by abutting valve surface (D). *Fragilariopsis pseudonana* forming colony by abutting valve surfaces (E-G). *Chaetoceros criophilum* (H, I). *Distephanus speculum* (J).





**Fig. 6.** Contours of carbon biomass on total phytoplankton (A, B), total phytoflagellates (C, D) and total diatoms (E, F) in the upper 100 m along the transects 1 and 2. The bottom contour (G, H).

(motile form), *Fragilariopsis pseudonana*, *Chaetoceros criophilum* and *Rhizosolenia antennata fo. semispina*. Recall that the total distance of the two transects between the southernmost station and the northernmost station was about 220 km. Discrete total phytoplankton carbon from 144 water samples collected in the upper 100 m ranged from  $<1$  to  $>75 \mu\text{g}\cdot\text{C}\cdot\text{l}^{-1}$  (Fig. 6A, B). In both transects total phytoplankton carbon was concentrated in the upper 50 m waters. The elevated concentrations were coincident with the hydrographic features such as higher temperature and lower salinity (e.g. See figs 2, 3 in Kang et al., 1993b).

Overall, phytoflagellates and diatoms showed different distributional pattern. Phytoflagellates were generally observed in highest carbon values ( $40\text{--}70 \mu\text{g}\cdot\text{C}\cdot\text{l}^{-1}$ ) near Snow and Livingston Islands (Stations 8, 9, 16–18) in Bransfield Strait region (Fig. 6C, D). On the other hand, diatoms were concentrated in the northern portion of the study area located in the Drake Passage with range of  $20\text{--}40 \mu\text{g}\cdot\text{C}\cdot\text{l}^{-1}$  (Fig. 6E, F).

*Cryptomonas* sp. that dominated most of the samples in Bransfield Strait region was concentrated in the upper 50 m in both transects (20–50

$\mu\text{g}\cdot\text{C}\cdot\text{l}^{-1}$ ; see Fig. 7A, B). Lower carbon ( $<10 \mu\text{g}\cdot\text{C}\cdot\text{l}^{-1}$ ) was observed at the Drake Passage stations (Stations 10, 11, 19–21) and the Bransfield Strait stations (Stations 2–7). The other important phytoflagellate, *Phaeocystis* sp. (motile form) showed similar distribution pattern like *Cryptomonas* sp., but more restricted in distribution around Low and Smith Island station (Stations 8, 9, 16–18; see Fig. 7C, D). The maximal carbon values ranged between 10 and  $15 \mu\text{g}\cdot\text{C}\cdot\text{l}^{-1}$ .

The dominant diatom species, *Fragilariopsis pseudonana*, *Chaetoceros criophilum* and *Rhizosolenia antennata fo. semispina* showed different patterns of distribution as compared to the phytoflagellates (Fig. 7E–J). These species were concentrated in the upper 80 m at the Drake Passage stations (Stations 9–11, 18–21), with *F. pseudonana* present at carbon as high as  $>25 \mu\text{g}\cdot\text{C}\cdot\text{l}^{-1}$  (Fig. 7E, F) and *R. antennata fo. semispina* at  $>20 \mu\text{g}\cdot\text{C}\cdot\text{l}^{-1}$  (Fig. 7M). Especially, *R. antennata fo. semispina* was observed the maximum carbon value in the deeper samples ( $\sim 80$  m).

## DISCUSSION

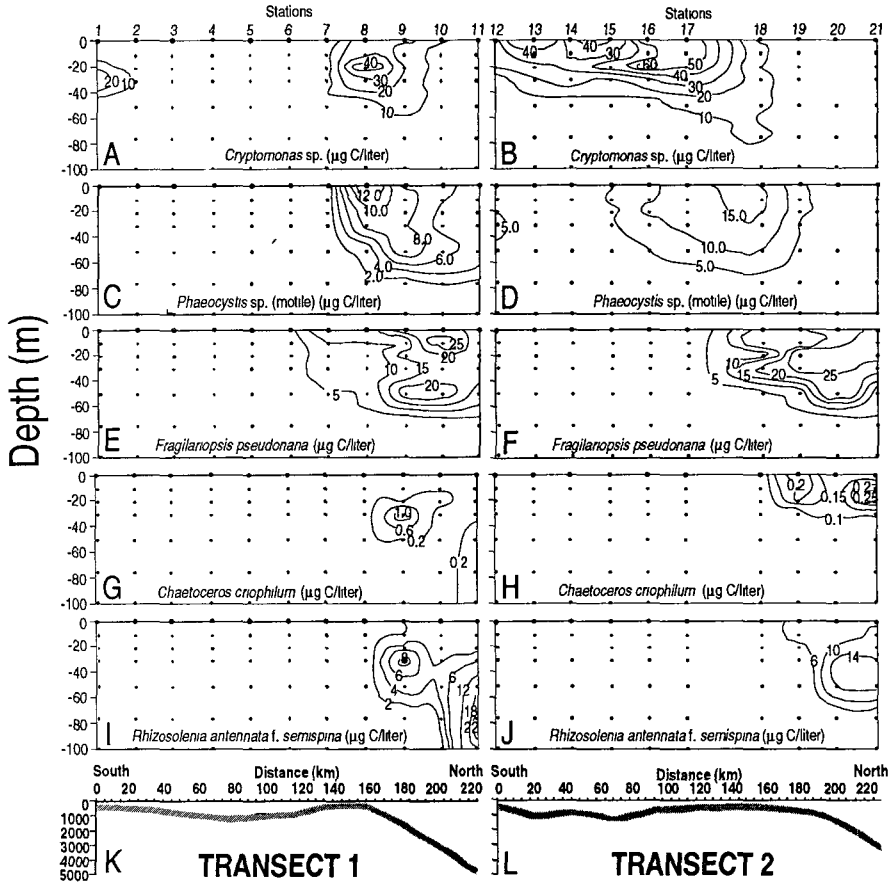


Fig. 7. Contours of the dominant phytoplankton species biomass in the upper 100 m along the transects 1 and 2. (A, B) *Cryptomonas* sp.; (C, D) *Phaeocystis* sp.; (E, F) *Fragilariopsis pseudonana*; (G, H) *Chaetoceros criophilum*; (I, J) *Rhizosolenia antennata* f. *semispina*; (K, L) the bottom contour.

A number of processes that affect phytoplankton distribution in Antarctic regions such as physical processes (e.g. fronts, eddies, interleaving) and biological processes (e.g. sinking, grazing) are considered to be independent of those that influence growth such as temperature, light (including variations induced by ice cover and the vertical movements of water), nutrient supply ("new" nutrients brought to the euphotic zone from depth by vertical transport and "regenerated" nutrients produced by the heterotrophic activities), organic growth factors, and heavy metals (Smith and Sakshaug, 1990), but the phytoplankton species composition, biomass and mesoscale distribution at one point in space and time may result from the combination of these factors.

In an attempt to investigate the mesoscale spatial

patterns and relationships between sample depths and between stations, principal component analysis (PCA) was performed using carbon values of total phytoplankton, total phytoflagellates, total diatoms, *Cryptomonas* sp., *Phaeocystis* sp. (motile form), cysts, *Fragilariopsis pseudonana* and *Rhizosolenia antennata* fo. *semispina* as variables. The two plots in Fig. 8 (A, B) are identical but in Fig. 8A, the symbols represent the stations from which the samples came, while in Fig. 8B they represent relative depth. Relative depth 1 at a station is the shallowest. The circumscriptions are subjective but help to delineate the patterns and relationships between sample depths and between stations. Four groups emerge.

Group 1 consists of the surface and sub-surface samples from Stations 7, 10, 11 in transect 1 and

**Table 2.** Mean values of physical, chemical and biological variables of groups delineated from the PCA (Fig. 8). CHLA = chlorophyll a ( $\mu\text{g}\cdot\text{C}\cdot\text{l}^{-1}$ ), TP = total phytoplankton ( $\mu\text{g}\cdot\text{C}\cdot\text{l}^{-1}$ ), TPF = total phytoflagellates ( $\mu\text{g}\cdot\text{C}\cdot\text{l}^{-1}$ ), TD = total diatoms ( $\mu\text{g}\cdot\text{C}\cdot\text{l}^{-1}$ ), CRYPTO = *Cryptomonas* sp. ( $\mu\text{g}\cdot\text{C}\cdot\text{l}^{-1}$ ), PH = *Phaeocystis* sp. in motile state ( $\mu\text{g}\cdot\text{C}\cdot\text{l}^{-1}$ ), CYST = siliceous cyst ( $\mu\text{g}\cdot\text{C}\cdot\text{l}^{-1}$ ), FP = *Fragilariopsis pseudonana* ( $\mu\text{g}\cdot\text{C}\cdot\text{l}^{-1}$ ), RHA = *Rhizosolenia anetennata* fo. *semispina*, NO3 = nitrate ( $\mu\text{M}$ ), PO4 = phosphate ( $\mu\text{M}$ ), SIO4 = silicate ( $\mu\text{M}$ ), TEMP = temperature ( $^{\circ}\text{C}$ ), SAL = salinity ( $\text{‰}$ ), DEN = density ( $\text{sigma-t}$ )

		CHLA	TP	TPF	TD	CRYPTO	PH	CYST	FP	RHA	NO3	PO4	SIO4	TEMP	SAL	DEN
All Stations	Minimum	0.010	0.337	0.313	0.000	0.000	0.000	0.000	0.000	0.000	8.580	0.870	7.400	0.024	33.573	26.876
	Maximum	1.720	79.901	79.227	53.316	76.360	17.936	1.306	38.326	22.280	39.320	3.880	68.030	2.364	34.312	27.541
	Mean	0.427	22.194	14.410	7.784	9.417	2.954	0.171	5.433	1.588	20.594	2.132	35.329	1.216	33.955	27.189
	Std Deviation	0.372	22.074	18.856	12.717	16.231	4.277	0.203	9.099	3.747	5.623	0.621	13.562	0.657	0.159	0.163
Group 1	Minimum	0.060	8.039	0.319	5.212	0.000	0.000	0.000	1.380	0.000	15.510	1.560	7.400	0.214	33.688	26.911
	Maximum	0.850	57.369	14.329	53.316	4.170	8.401	0.625	38.326	22.280	32.900	3.140	59.550	2.364	34.123	27.339
	Mean	0.387	31.630	5.512	26.118	0.886	2.656	0.158	17.713	6.352	23.176	2.182	24.585	1.739	33.823	27.046
	Std Deviation	0.198	13.562	4.009	12.440	1.124	2.828	0.169	9.948	5.648	5.180	0.412	11.964	0.583	0.118	0.130
Group 2	Minimum	0.010	0.337	0.313	0.000	0.000	0.000	0.000	0.000	0.000	8.580	0.870	15.060	0.024	33.743	27.043
	Maximum	1.720	25.693	25.693	8.597	22.413	7.680	1.306	7.972	3.180	39.320	3.880	68.030	1.990	34.312	27.541
	Mean	0.327	4.976	4.147	0.830	1.592	0.688	0.249	0.629	0.152	19.825	2.023	39.427	0.784	34.050	27.294
	Std Deviation	0.446	4.398	4.135	1.443	3.147	1.433	0.231	1.183	0.569	6.170	0.747	13.422	0.534	0.127	0.127
Group 3	Minimum	0.340	25.931	19.224	1.533	5.560	7.481	0.000	1.533	0.000	13.090	1.650	25.650	1.620	33.828	27.045
	Maximum	0.460	75.233	35.229	41.895	24.324	17.936	0.307	27.594	9.709	31.230	2.780	37.680	2.003	33.906	27.124
	Mean	0.390	51.090	28.654	22.436	14.672	11.859	0.065	16.948	2.864	21.452	2.146	30.713	1.858	33.845	27.057
	Std Deviation	0.037	16.887	5.302	12.852	6.599	4.054	0.098	9.251	3.888	5.705	0.358	4.124	0.137	0.024	0.025
Group 4	Minimum	0.170	10.130	10.130	0.000	4.587	0.000	0.000	0.000	0.000	14.010	1.450	22.900	1.021	33.573	26.876
	Maximum	1.200	79.901	79.227	14.564	76.360	14.840	0.245	11.242	0.000	28.300	3.510	64.150	2.036	34.116	27.333
	Mean	0.698	43.554	41.405	2.149	33.208	5.727	0.046	1.511	0.000	19.282	2.309	37.777	1.508	33.898	27.124
	Std Deviation	0.268	21.533	20.937	3.946	19.202	4.959	0.072	2.696	0.000	3.703	0.483	10.937	0.336	0.146	0.123

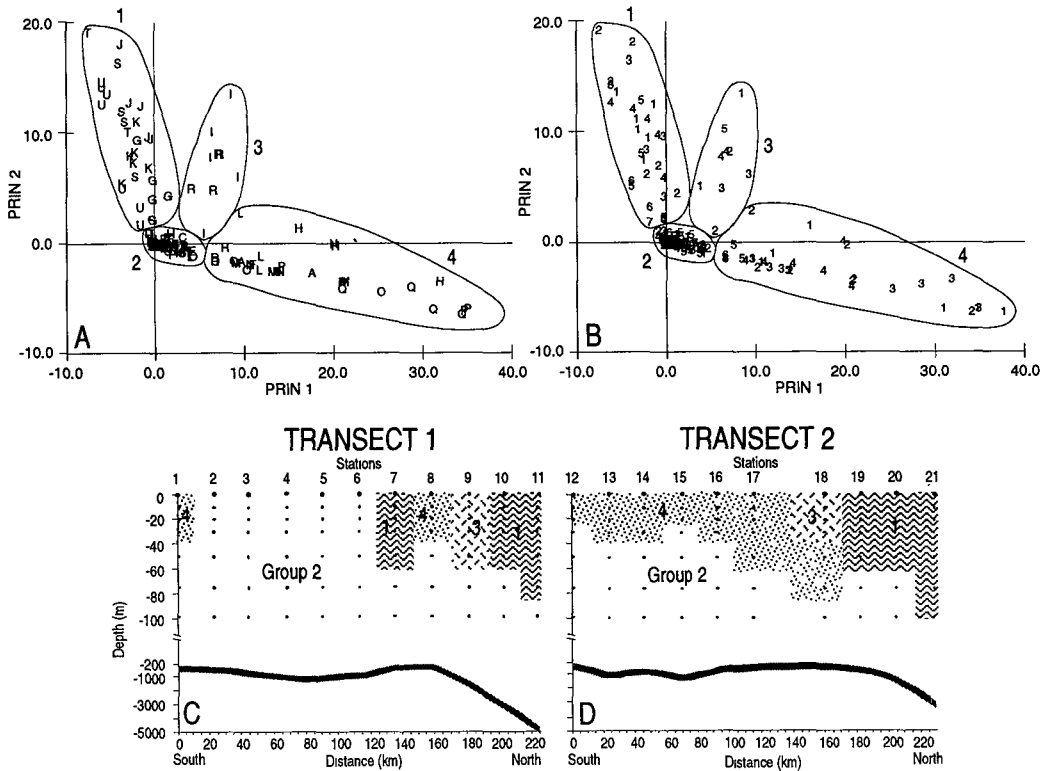


**Fig. 8.** Principal component analysis (PCA) using carbon values ( $\mu\text{g}\cdot\text{C}\cdot\text{l}^{-1}$ ) of eight phytoplankton species and groups as variables. (A) Stations from the 6th KARP cruise (A-K = stations in transect 1, where A = Station 1, K = Station 11, L-U = stations in transect 2, where L = Station 12, U = Station 21). (B) Relative depth, where 1 = shallowest sample at a station. Sample groups are subjectively encircled to facilitate visualization of patterns. Location of these groups in a two-dimensional section of study area (C, D).

Stations 19-21 in transect 2 located at the Drake Passage region (Fig. 8C, D), where we observed the highest mean carbon value of total diatoms ( $26 \pm 12 \mu\text{g}\cdot\text{C}\cdot\text{l}^{-1}$ ). It was about five times higher than the mean carbon value of total phytoflagellates ( $5.5 \pm 4.0 \mu\text{g}\cdot\text{C}\cdot\text{l}^{-1}$ ; see Table 2). *Fragilariopsis pseudonana* and *Rhizosolenia antennata* fo. *seminspina* were the major carbon contributors in the Group 1 samples. Mean density ( $\sigma\text{-t}$ ) of the water column in Group 1 samples was the lowest ( $27.05 \sigma\text{-t}$ ) due to the higher temperature ( $1.74 \pm 0.54^\circ\text{C}$ ) and the lower salinity ( $33.82 \pm 0.12\text{‰}$ ). Minimum concentrations of silicate ( $24.59 \pm 11.96 \mu\text{M}$ ) were observed in this Group (Table 2), indicating that the silicate was affected strongly by *in situ* uptake by diatoms.

Group 2 includes samples with the lowest phytoplankton carbon value (mean of  $\sim 5 \mu\text{g}\cdot\text{C}\cdot\text{l}^{-1}$ ). It was about 5 times lower than mean total carbon phyto-

plankton carbon ( $\sim 22 \mu\text{g}\cdot\text{C}\cdot\text{l}^{-1}$ ). The samples in Group 2 were characterized by unstable water condition with the lowest mean temperature ( $0.78 \pm 0.53^\circ\text{C}$ ) and the highest salinity ( $34.05 \pm 0.13\text{‰}$ ), hence the highest  $\sigma\text{-t}$  value ( $27.29 \pm 0.13$ ) is about 0.25  $\sigma\text{-t}$  unit differences compared to the lowest density waters in Group 1 samples (Table 2).

Group 3 consists of surface samples in Station 9 in transect 1 and Station 18 in transect 2 (Fig. 8). The samples in Group 3 seem to be in transitional condition between diatom-dominated area (Group 1 samples in the Drake Passage area) and phytoflagellate-dominated area (remaining samples in the Bransfield Strait region). The highest mean total phytoplankton carbon was observed ( $51.1 \pm 16.9 \mu\text{g}\cdot\text{C}\cdot\text{l}^{-1}$ ). Diatoms and phytoflagellates accounted for  $22.4 \pm 12.9 \mu\text{g}\cdot\text{C}\cdot\text{l}^{-1}$  and  $28.7 \pm 5.3 \mu\text{g}\cdot\text{C}\cdot\text{l}^{-1}$ , respectively. *Cryptomonas* sp., *Phaeocystis* sp.

**Table 3.** Species-specific growth rate of various Antarctic marine phytoplankton dependent on temperature

Species	Growth rate (div. day <sup>-1</sup> )	Temperature (°C)	Irradiance ( $\mu\text{Einst}\cdot\text{m}^{-2}\cdot\text{s}^{-1}$ )	Reference
<i>Chaetoceros neglectus</i>	0.71-0.95	3.5°	100	Buma et al. (1991)
<i>Chaetoceros</i> spp.	0.68	3.5°	100	Buma et al. (1991)
<i>Corethron criophilum</i>	0.67-0.68	3.5°	100	Buma et al. (1991)
<i>Nitzschia fragilaria</i>	0.44-0.66	3.5°	100	Buma et al. (1991)
<i>Nitzschia seriata</i>	0.54	3.5°	100	Buma et al. (1991)
<i>Rhizosolenia</i> spp.	0.52	3.5°	100	Buma et al. (1991)
<i>Thalassiosira</i> spp.	0.36	3.5°	100	Buma et al. (1991)
<i>Thalassiothrix</i> sp.	0.36-0.50	3.5°	100	Buma et al. (1991)
<i>Chaetoceros criophilum</i>	0.25-0.40	0°	160	Sommer (1989)
<i>Corethron criophilum</i>	0.36-0.46	0°	160	Sommer (1989)
<i>Eucampia antarctica</i>	0.35-0.41	0°	160	Sommer (1989)
<i>Fragilariopsis cylindrus</i>	0.57-0.75	0°	160	Sommer (1989)
<i>Fragilariopsis kerguelensis</i>	0.51-0.60	0°	160	Sommer (1989)
<i>Nitzschia seriata</i>	0.47-0.60	0°	160	Sommer (1989)
<i>Odontella weissflogii</i>	0.39-0.52	0°	160	Sommer (1989)
<i>Phaeocystis pouchetii</i>	0.69-0.73	0°	160	Sommer (1989)
<i>Pyramimonas</i> sp.	0.43-0.75	0°	160	Sommer (1989)
<i>Proboscia alata</i>	0.39-0.58	0°	160	Sommer (1989)
<i>Rhizosolenia antenata</i>	0.31-0.37	0°	160	Sommer (1989)
<i>Rhizosolenia truncata</i>	0.37-0.58	0°	160	Sommer (1989)
<i>Thalassiosira antarctica</i>	0.37-0.52	0°	160	Sommer (1989)
<i>Thalassiosira subtilis</i>	0.43-0.49	0°	160	Sommer (1989)
<i>Thalassiothrix longissima</i>	0.37-0.45	0°	160	Sommer (1989)
<i>Asteromphalus</i> spp.	0.67-0.84	-1°	45	Spies (1987)
<i>Chaetoceros dictyochaeta</i>	0.57	-1°	45	Spies (1987)
<i>Chaetoceros</i> spp.	0.54-1.33	-1°	45	Spies (1987)
<i>Coscinodiscus</i> spp.	0.64-0.71	-1°	45	Spies (1987)
<i>Eucampia antarctica</i>	0.39-1.15	-1°	45	Spies (1987)
<i>Fragilariopsis</i> spp.	0.60-1.09	-1°	45	Spies (1987)
<i>Nitzschia</i> spp.	0.41-1.23	-1°	45	Spies (1987)
<i>Odontella</i> spp.	0.42	-1°	45	Spies (1987)
<i>Rhizosolenia</i> spp.	0.48-0.70	-1°	45	Spies (1987)
<i>Thalassiosira</i> spp.	0.38-1.16	-1°	45	Spies (1987)
<i>Chaetoceros deflandrei</i>	0.33-0.88	2° to 15°	46 to 220	Fiala and Oriol (1990)
<i>Corethron criophilum</i>	0.13-0.38	0° to 6°	46 to 220	Fiala and Oriol (1990)
<i>Fragilariopsis cylindrus</i>	0.27-0.86	0° to 9°	46 to 220	Fiala and Oriol (1990)
<i>Fragilariopsis kerguelensis</i>	0.30-0.80	0° to 7°	46 to 220	Fiala and Oriol (1990)
<i>Nitzschia turgiduloides</i>	0.25-0.71	1° to 8°	46 to 220	Fiala and Oriol (1990)
<i>Stellarima microtrias</i>	0.42-0.85	1° to 7°	46 to 220	Fiala and Oriol (1990)
<i>Synedra</i> sp.	0.31-0.56	1° to 7°	46 to 220	Fiala and Oriol (1990)

(motile form) and *Fragilariopsis pseudonana* were all important carbon contributor in this Group. In spite of the high carbon biomass, relatively high nutrients were observed (nitrate, 21.5  $\mu\text{M}$ ; phosphate, 2.15  $\mu\text{M}$ ; silicate, 30.7  $\mu\text{M}$ ). Vertical stabi-

ty of water column in this Group 3 was high (mean of 27.05 sigma-t) due to the lower salinity (33.85 ‰) and higher temperature (1.86°C). The mean temperature (1.86  $\pm$  0.14°C) was the highest. When compared to the lowest temperature waters in

Group 2 ( $0.784 \pm 0.53^\circ\text{C}$ ), it was about  $1.1^\circ\text{C}$  higher in this area.

Group 4 includes samples that phytoflagellates were predominant relatively and absolutely ( $\sim 41.4 \pm 20.9 \mu\text{g}\cdot\text{C}\cdot\text{l}^{-1}$ ). It was about 19 times higher carbon value compared to mean total diatom carbon ( $2.1 \pm 3.9 \mu\text{g}\cdot\text{C}\cdot\text{l}^{-1}$ ). *Cryptomonas* sp. ( $33.2 \pm 19.2 \mu\text{g}\cdot\text{C}\cdot\text{l}^{-1}$ ) and *Phaeocystis* sp. ( $5.73 \pm 4.96 \mu\text{g}\cdot\text{C}\cdot\text{l}^{-1}$ ) were dominant species in this Group. Although mean density of waters was a little bit higher ( $27.12 \pm 0.12 \text{ sigma-t}$ ) than diatom-dominated samples in Groups 1 and 3, stability of water column was high enough for increased phytoplankton carbon due to higher temperature ( $1.51 \pm 0.34^\circ\text{C}$ ) and low salinity ( $33.9 \pm 0.15 \text{ ‰}$ ). The difference between the diatom-dominated waters and the phytoflagellate-dominated waters seems to be caused by physical mechanisms such as vertical stability and fine-scale temperature changes.

The PCA analysis using the phytoplankton species carbon values showed our samples in the western Bransfield Strait region to cluster by samples and stations which are a similar patterns between the phytoplankton species biomass and physical factors. In general, there was a strong relationship between the physical and biological structure. Physical mechanisms such as fine-scale temperature differences during the study period seem to play an important role to control phytoplankton growth and distribution. Table 3 shows species-specific growth rate of various Antarctic marine phytoplankton dependent on temperature.

Goldman and Carpenter (1974) showed that complex interactions between the nutrient uptake and growth parameters at different temperatures can lead to complex competitive interactions between species and thereby resulting in (or leading to) change in phytoplankton assemblages. Our results furnish support for the view that mesoscale differences in phytoplankton species composition, standing stock and distribution is related to regional differences on stabilization of the upper water column by low salinity and to fine-scale differences of temperatures.

## ACKNOWLEDGEMENTS

This work was supported by the Ministry of Science and Technology in Korea (Grant BSNP

00183-604-7). We are indebted to the crew of R.V. *Omnuri*, who were most helpful in all our shipboard operations. We thank S. Lee, Y.-C., Kang, C.Y., Kang, S.H., Ham, S.H., Kim and S.J. Pae for their excellent assistance with sample collections; J.S. Kang for sample preparation; S. Kim, I.-Y. Ahn, and H. Chung for their support and helpful suggestions.

## REFERENCES

- Becquevort, S., S. Mathot and C. Lancelot. 1992. Interactions in the microbial community of the marginal ice zone of the northwestern Weddell Sea through size distribution analysis. *Polar Biol.* **12**: 211-218.
- Buma, A.G.J., H.J.W. de Baar, R.F. Nolting and A.J. van Bennekom. 1991. Metal enrichment experiments in the Weddell-Scotia Seas: Effects of iron and manganese on various plankton communities. *Limnol. Oceanogr.* **36**: 1865-1878.
- Crumpton, W.G. 1987. A simple and reliable method for making permanent mounts of phytoplankton for light and fluorescence microscopy. *Limnol. Oceanogr.* **32**: 1154-1159.
- Dykstra, M.J. 1992. Biological Electron Microscopy. Theory, Techniques, and Troubleshooting. Plenum Press, New York and London. 360 pp.
- Fiala, M. and L. Oriol. 1990. Light-temperature interactions on the growth of Antarctic diatoms. *Polar Biol.* **10**: 629-636.
- Fryxell, G.A. and G.A. Kendrick. 1988. Austral spring microalgae across the Weddell Sea ice edge: Spatial relationships found along a northward transect during AMERIEZ 83. *Deep-Sea Res.* **35**: 1-20.
- Garrison, D.L. and K.R. Buck. 1985. Sea-ice algal communities in the Weddell Sea: Species composition in ice and plankton assemblages. In, Gary, J. S. and M.E. Christiansen (eds.). Marine Biology of Polar Regions and Effects of Stress on Marine Organisms. John Wiley, New York. pp.103-122.
- Goldman, J.C. and E.J. Carpenter. 1974. A kinetic approach to the effect of temperature on algal growth. *Limnol. Oceanogr.* **19**: 756-766.
- Graedel, T.E. and P.J. Crutzen. 1993. Atmospheric Change: An Earth System Perspective. Freeman Co., New York. 446 pp.
- Hasle, G.R. 1965a. *Nitzschia* and *Fragilariopsis* species studied in the light and electron microscopes. II. The group *Pseudonitzschia*. *Skr. Norske Vidensk.-Akad. Oslo, I. Mat. -Naturvidensk. Kl., N.S.* **18**: 1-45.
- Hasle, G.R. 1965b. *Nitzschia* and *Fragilariopsis* species in the light and electron microscopes. III. The genus

- Fragilariopsis*. *Skr. Norske Vidensk.-Akad. Oslo, I. Mat.-Naturvidensk. Kl., N.S.* **21**: 1-49.
- Hasle, G.R. 1972. *Fragilariopsis* Hustedt as a section of the genus *Nitzschia* Hassall. *Nova Hedwigia* **39**: 111-119.
- Hasle, G.R. 1993. Nomenclatural notes on marine planktonic diatoms. The family Bacillariaceae. *Nova Hedwigia* **106**: 315-321.
- Hofmann, E.E., C.M. Lascara and J.M. Klinck. 1992. Palmer LTER: Upper-ocean circulation in the LTER region from historical sources. *Antarct. J. U.S.* **27**: 239-241.
- Kang, S.-H. 1989. Diatom species composition and abundance in water column assemblages from five drill sites in Prydz Bay, Antarctica, Ocean Drilling Program Leg 119: Distributional patterns. M.S. Thesis. Texas A&M University. 139 pp.
- Kang, S.-H. and G.A. Fryxell. 1991. Most abundant diatom species in water column assemblages from five ODP Leg 119 drill sites in Prydz Bay, Antarctica: Distributional patterns. *In*, Barron, J. and B. Larsen (eds.). Proceedings of the ODP Scientific Results, 119. (Ocean Drilling Program) College Station, TX. pp. 645-666.
- Kang, S.-H. and G.A. Fryxell. 1992. *Fragilariopsis cylindrus* (Grunow) Krieger: The most abundant diatom in the water column assemblages in Antarctic marginal ice-edge zones. *Polar Biol.* **12**: 609-627.
- Kang, S.-H. and G.A. Fryxell. 1993. Phytoplankton in the Weddell Sea, Antarctica: composition, abundance and distribution in the water-column assemblages of the marginal ice-edge zone during austral autumn. *Mar. Biol.* **116**: 335-348.
- Kang, S.-H., G.A. Fryxell and D.L. Roelke. 1993a. *Fragilariopsis cylindrus* compared with other species of the diatom family Bacillariaceae in Antarctic marginal ice-edge zones. *Nova Hedwigia* **106**: 335-352.
- Kang, S.-H., M.S. Suk, C.S. Chung and S.Y. Nam. 1993b. Phytoplankton composition, biomass and distribution in the western Bransfield Strait region, Antarctica: relationship to hydrography and nutrients. Korea Ocean Research and Development Institute Report (BSPG 00169-5-485-7). pp. 403-491.
- Karentz, D., J.E. Cleaver and D.L. Mitchell. 1991. Cell survival characteristics and molecular responses of Antarctic phytoplankton to ultraviolet-b radiation. *J. Phycol.* **27**: 326-341.
- Kopczynska, E.E. 1992. Dominance of microflagellates over diatoms in the Antarctic areas of deep vertical mixing and krill concentrations. *J. Plankton Res.* **14**: 1031-1054.
- Leventer, A. 1991. Sediment trap diatom assemblages from the northern Antarctic Peninsula region. *Deep-Sea Res.* **38**: 1127-1143.
- Marchant, H.J. and A. Davidson. 1992. Possible impacts of ozone depletion on trophic interactions and biogenic vertical carbon flux in the Southern Ocean. *In*, Weller, G., C.L. Wilson and B.A. Severin (eds.). Proceedings of the International Conference on the Role of Polar Regions in Global Change. Geophysical Institute, Fairbanks. pp. 631-635.
- Medlin, L.K. and J. Priddle. 1990. Polar Marine Diatoms. British Antarctic Survey, Natural Environment Research Council, Cambridge. 214 pp.
- Round, F.E., R.M. Crawford and D.G. Mann. 1990. The diatoms: Biology and morphology of the genera. Cambridge University Press, Cambridge. 747 pp.
- Smayda, T.J. 1978. From phytoplankton to biomass. *In*, Sournia, A. (ed.). Monographs on Oceanic Methodology. 6. Phytoplankton Manual. UNESCO, Paris. pp. 273-279.
- Smith, R.C., B.B. Prézelin, K.S. Baker, R.R. Bidigare, N.P. Bouche, T. Coley, D. Karentz, S. MacIntyre, H.A. Matlick, D. Menzies, M. Ondrusek, Z. Wan and K.J. Waters. 1992. Ozone depletion: Ultraviolet radiation and phytoplankton biology in Antarctic waters. *Science* **255**: 952-959.
- Smith, W.O., Jr. and E. Sakshaug. 1990. Polar phytoplankton. *In*, Smith, W. O. Jr. (ed.). Polar Oceanography, Part B: Chemistry, Biology and Geology. Academic Press, Inc., San Diego. pp. 477-525.
- Sommer, U. 1989. Maximal growth rates of Antarctic phytoplankton: Only week dependence on cell size. *Limnol. Oceanogr.* **34**: 1109-1112.
- Spies, A. 1987. Growth rates of Antarctic marine phytoplankton in the Weddell Sea. *Mar. Ecol. Prog. Ser.* **41**: 267-274.